Genes & Diseases (2023) 10, 719–722

Available online at www.sciencedirect.com

ScienceDirect

journal homepage: www.keaipublishing.com/en/journals/genes-diseases

RAPID COMMUNICATION

FXR suppresses colorectal cancer by inhibiting the Wnt/β-catenin pathway via activation of TLE3

Colorectal cancer (CRC) is the third most common and lethal cancer worldwide.[1] Farnesoid X receptor (FXR) is a regulator of bile acid (BA) homeostasis and its expression is inversely correlated with the incidence of CRC.[2,3] Moreover, our recent study discovered that dietary factors and dysregulated Wnt signaling independently alter BA profiles, some of which antagonize intestinal FXR, such as Tauro-β-muricholic acid (T-βMCA) and deoxycholic acid (DCA).[2] These antagonistic BAs drove malignant transformations in Lgr5-expressing (Lgr5^{+}) intestinal stem cells (ISCs), which promoted an adenoma-to-adenocarcinoma progression.[2] Conversely, FXR agonists restored BAs homeostasis and curtailed CRC progression.[2] However, the precise mechanism of FXR inhibiting Wnt signaling remains unclear, prompting us to investigate FXR's targets in Wnt pathway, especially in ISCs.

Almost all CRC subtypes are characterized by a hyperactive Wnt pathway which is critical for cell proliferation and cancer initiation.[1] Transducin-like enhancer of split (TLE) proteins belong to a family of transcriptional corepressors that widely express in metazoans.[1] We first examined TLE3 by IHC in tumors versus normal tissues[4, 6]. Indeed, TLE3's expression was significantly higher in normal tissues (Fig. 1A) but downregulated in tumors (Fig. 1B; Fig.S1A). We also noticed a gradual decrease of TLE3 (Fig. S1B) and increase of methylation (Fig. S1C) along tumor progression, which correlates with FXR expression. Notably, TLE3 is strongly associated with adenoma formation by gene-set enrichment analysis (GSEA) of The Cancer Genome Atlas (TCGA) (Fig. 1C).

To further understand the association between FXR and TLE3, we examined their expression in normal tissues and CRC tumors. Indeed, FXR expression was profoundly declined in tumors (Fig. 1D). However, in combined normal and tumor samples, FXR and SHP only showed a modest positive correlation with TLE3 (Fig. S1D). Even Hes1, a known gene repressed by TLE3,[1] displayed a modest correlation (Fig. S1D). Notably, both FXR and TLE3 express low in advanced tumors. Thus, we observed a strong positive correlation between FXR and TLE3 in normal colorectal tissues (Fig. 1E). We then validated it in normal tissues from combined TCGA and GTEx databases (Fig. S1E) and in small intestinal samples from GTEx, which commonly have higher FXR expression and more active Wnt (Fig. S1F). We also observed larger differences in TLE3 and FXR expression between normal versus tumors in pooled samples from GTEx (Fig. S1G). In addition, we also evaluated the prognostic significance of FXR, TLE3, and HES1 in different stages (Fig. S2A, B). CRC patients with higher FXR expression had better survival in all the stages, whereas patients with higher TLE3 only showed better survival in early stages (Fig. S2). Collectively, these data suggested that FXR and TLE3 have a positive correlation in normal intestine, whose dysregulation may contribute to adenoma formation.

To validate Fxr truly regulates Tle3, we first examined Tle3 expression in FXRKO mice. Compared to WT, Tle3 does not express in cell nucleus (Fig. 1E; Fig. S3A), and its expression also reduced in FXRKO mice (Fig. 1G). To further validate FXR's regulatory role, we used FXR agonistic and antagonistic ligands on Apc$^{Min/+}$ intestinal organoids (Fig. S3B).[2] Indeed, Fxr agonists like FexD, OCA, and GW4064 significantly elevated Tle3 expression, while antagonists like Dy268, T-βMCA, and DCA have no effects (Fig. S3C). Oppositely, we observed reduced expression of *Ccnd1*, *Lgr5*, and *Ascl2* upon agonists' treatment but not with antagonists (Fig. S3C). Additionally, decreased levels of *Tle3* were observed in Apc$^{Min/+}$ mice but increased upon FexD (Fig. 1H). We also observed increased expression of *Ccnd1*, *Lgr5*, and *Ascl2* in Apc$^{Min/+}$ mice, whereas reduced upon FexD (Fig. 1H). Interestingly, we noticed immunostaining of Tle3 almost diminished inside tumor but only scarcely present at the outer surface in Apc$^{Min/+}$ mice, whereas FexD profoundly increased it, especially in crypts

Peer review under responsibility of Chongqing Medical University.

https://doi.org/10.1016/j.gendis.2022.09.006

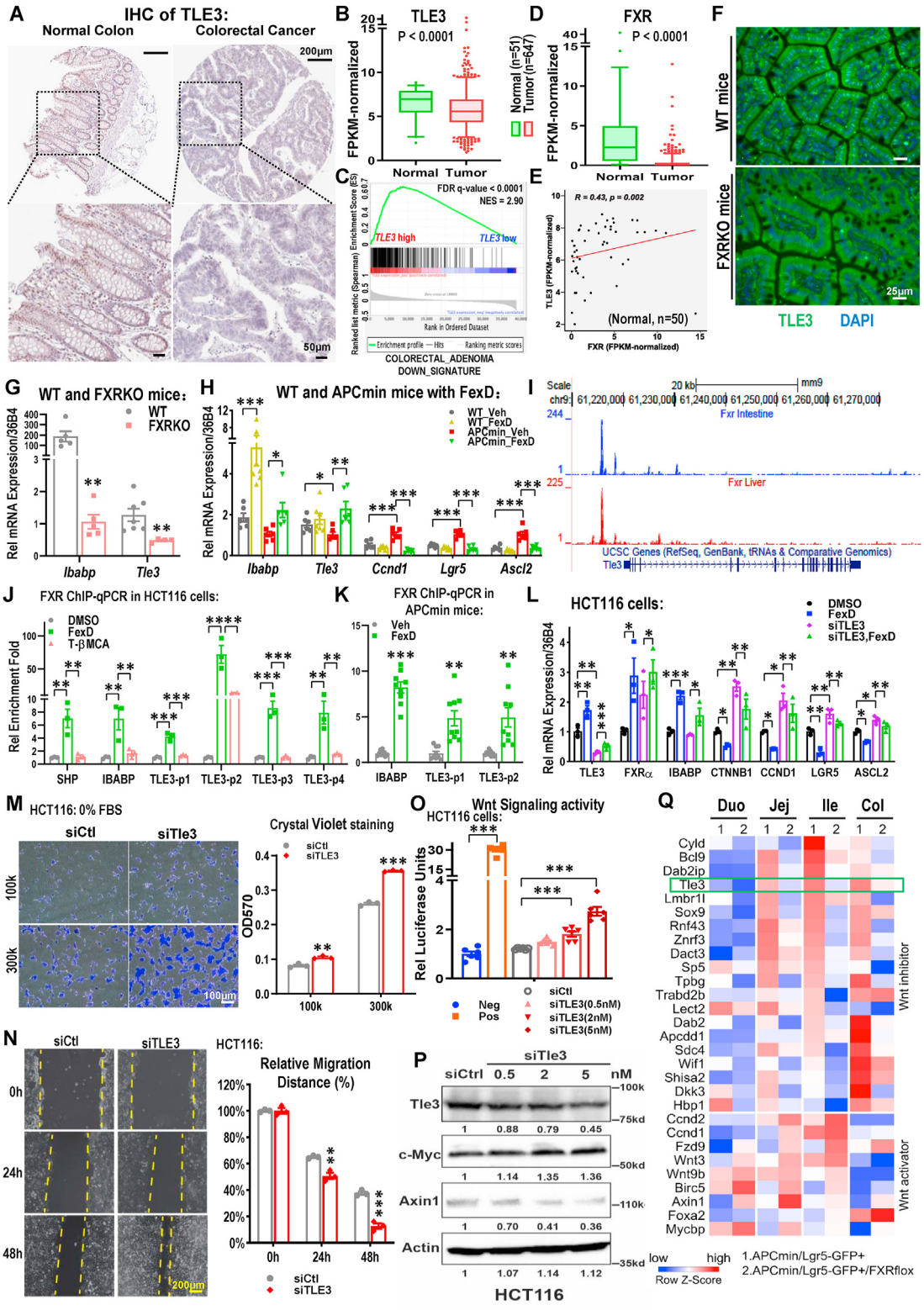

Fig. 1 FXR inhibits Wnt/β-catenin signaling pathway through activation of TLE3. **(A)** Representative Immunohistochemistry (IHC) staining image of TLE3 in normal and colon cancer tissue samples from Human Protein Atlas in TCGA cohort, Scale bar 200 μm upper panel, 50 μm upper panel. **(B)** The expression levels of TLE3 in normal colon tissues ($n = 51$) versus primary tumors ($n = 647$) from COAD and READ cohort of TCGA data. Box and whiskers graph is presented within 5–95 percentile, with medium number shown in the middle. **(C)** Gene-set enrichment analysis (GSEA) of TLE3 in colorectal cancer patients from TCGA. Representative GSEA plots indicated that TLE3 expression is positively associated with downregulated signature genes in Colorectal adenoma formation pathway gene sets, with significant cut-off defined by false discovery rate (FDR) and normalized enrichment score (NES) of TLE3 are indicated. **(D)** The expression levels of FXR in normal colon tissues ($n = 51$) versus primary tumors ($n = 647$) from COAD and READ

(Fig. S3D). All together, these data revealed the potential role of Tle3 and Fxr in ISCs' proliferation and tumorigenesis. To investigate the regulatory role of Fxr, we examined the ChIP-seq data of Fxr in both intestine and liver. FXR binding peaks were detected on the promoter region of Tle3 gene (Fig. 1I), with potential FXR binding motifs identified on both mouse and human Tle3 (Fig. S3E). FXR, therefore, may directly regulate Tle3. To confirm this, Fxr ChIP-qPCR analyses were performed in CRC cells with treatment of FexD and T-βMCA. FexD increased FXR occupancy at Shp and Ibabp, also at Tle3 confirmed with several primers (Fig. 1J; Fig. S3F), but not upon T-βMCA. Additionally, FexD also increased FXR occupancy in $Apc^{Min/+}$ mice (Fig. 1K), revealing FXR upregulated *Tle3 in vivo*.

To investigate the mechanism behind, we initially examined the effect of silencing Tle3 in HCT116. As shown in Figure 1L, siTLE3 elicited significant increased expression of *CCND1*, *LGR5*, *ASCL2*, and *CTNNB1*, whereas FexD markedly inhibited their expression. Moreover, the effects of FexD and T-βMCA are greatly compromised upon siTLE3 (Fig. 1L). Of note, FexD treatment after siTLE3 demonstrated dramatic changes compared to FexD only (Fig. 1L), indicating FexD's impact is compromised upon Tle3 silencing. To further assess Tle3's effects on cell viability and proliferation, we performed the CellTiter-Glo assay to measure ATP generation in cells after treatment of GW4064 or siTLE3. HCT116 viabilities were dose-dependently decreased upon dose-dependent increase of GW4064 (Fig. S3H), whereas their viabilities were dose-dependently increased upon dose-dependently increased of siTLE3 (Fig. S3I). Moreover, the opposite effects on cell growth were also measured by crystal violet assay (Fig. 1M; Fig. S4A-B). Moreover, wound healing assays showed that the migratory and invasive capabilities of HCT116 were decreased by GW4064 but increased by siTLE3 (Fig. 1N; Fig. S4C). Taken together, these results suggested Tle3 plays an important role in repressing tumorigenicity and metastasis.

TLE exerts long-range repression on a variety of transcriptional factors, including Tcf/Lef, Hes, Runx, Myc, which repress Wnt signaling.[1,4,5] We next investigated how FXR might modulate the Wnt via TLE3. Silence of Tle3 activated the Wnt signaling, as determined by TOPflash activity (Fig. 1O). Nonetheless, Western-blot analysis revealed that silencing of Tle3 or GW4064 treatment changed the expression of Wnt effectors, like Axin1 and c-Myc (Fig. 1P; Fig. S4D). Furthermore, we examined the Tle3 level, Wnt and Notch signaling in pooled sorted ISCs of FXR ISCs-specific deleted $APC^{min/+}$ mice.[2] Consistent with FXR limiting ISCs' proliferation, decreased expression of Tle3 and Wnt inhibitors and increase of Wnt activators were seen in Lgr5+ and Lgr5-cells from these mice (Fig. 1Q; Fig. S4E), demonstrating that even short-term knockdown of FXR is enough to inhibit TLE3 and abolish its repression. Interestingly, we observed increased levels of Notch inhibitors and decreased levels of Notch activators in $Lgr5^{+}$ and $Lgr5^{-}$ cells from these mice (Fig. S4E), suggesting knockdown of FXR in ISCs attenuated Notch and allowed for high levels of Wnt. To further validate TLE3 as a dual-functional switch, we analyzed TLE3 expression by GSEA in TCGA. Indeed, TLE3 was strongly associated with Wnt and

cohort of TCGA data. Box and whiskers graph is presented within 5–95 percentile, with medium number shown in the middle. **(E)** Correlation between gene expression of *TLE3* and *FXR* genes in normal colorectal tissues from TCGA RNA-seq database ($n = 50$). **(F)** Immunofluorescent staining of Tle3 expression (green) in intestine section of WT and FXRKO mice, with the nucleus counterstained with DAPI (blue). Scale bar 25 μm. **(G)** The expression of *Tle3* and Fxr downstream targets (*Ibabp*) are reduced in FXRKO mice, compared with WT mice. **(H)** The expression of *Tle3*, Fxr target gene (*Ibabp)*, cell cycle gene (*Ccnd1*), intestinal stem cell (ISCs) signature genes (*Lgr5* and *Ascl2*) were measured by RT-qPCR in WT and $Apc^{Min/+}$ mice, a classic CRC mouse model, on normal diet treated with FXR agonists, Fexaramine D (FexD) from 8 to 16 weeks old. **(I)** Histogram of FXR binding sites at the promoter region of Tle3 genes from both intestine and liver FXR ChIP-seq data. The *y*-axis displays the peak value, and the *x*-axis shows the chromosomal location of the gene. The top panel (displayed in red) represents FXR binding in liver, and the bottom panel (displayed in blue) represents FXR binding in intestine. TLE3 is displayed above the chromosome-scale are oriented in the sense directions (right arrow). **(J)** HCT116 cells were treated with FXR agonistic drug, FexD and FXR antagonist natural bile acids, T-βMCA for 4h. Pooled cells were collected, and ChIP assays were performed. Occupancy of FXR at SHP, IBABP, TLE3 promoter regions were detected by q-PCR analysis. **(K)** $Apc^{Min/+}$ mice were treated with FexD or vehicle for 6 h, intestines were collected, and ChIP assays were performed. Occupancy of Fxr at Ibabp and Tle3 promoter regions were detected by q-PCR analysis. **(L)** HCT116 cells were transiently transfected with pooled siRNA of TLE3 (siTLE3) and Control (siCTL) for 20 h, then treated with FXR agonistic drug, FexD and FXR antagonist natural bile acids, T-βMCA for 4h. The expression of TLE3, FXR and its target genes (*FXR*, *IBABP*), Wnt signaling gene (*CTNNB1*), cell cycling gene (*CCND1*), intestinal stem cell markers (*LGR5*, *ASCL2*) were measured by RT-qPCR. **(M)** Knockdown of TLE3 by siTLE3 promotes HCT116 cell growth and proliferation, as determined by Crystal violet assay. Representative phase-contrast images were displayed, Scale bar 100 μm. **(N)** Silence of TLE3 by siTLE3 increased migratory capabilities of HCT116 cells. Wound healing assay was performed, and representative images are shown. Scale bar 200 μm. **(O)** Knockdown of TLE3 by siTLE3 activates Wnt signaling, as measured by Cignal TCF/LEF luciferase reporter assay, with provided negative and positive control. **(P)** HCT116 cells were knocked down by siTLE3 and control siRNA. Western blot analysis was formed to measure the key Wnt signaling pathway-related markers (TLE3, c-MYC, AXIN1). Band intensities were quantified by image J and labeled below each band. **(Q)** Heatmap showing relative gene expression of Wnt signaling inhibitors and activators in Lgr5-GFP + stem cells with or without FXR conditional knockdown. Lgr5-GFP + cells were isolated from different intestinal segments of $APC^{min/+}$/Lgr5-GFP, $APC^{min/+}$/Lgr5-GFP/FXRflox, (Lgr5-GFP + high cells—Intestinal Stem cells, were isolated were pooled from six mice 1 week after tamoxifen treatment). $n = 3–9$/group. Experiments were independently replicated twice, and representative data are shown as the mean ± SEM. *p*-values are computed with Student's unpaired *t*-test or one sample Wilcoxon test, or one-way ANOVA test followed by multiple comparisons. * FXRKO or $Apc^{Min/+}$ versus WT, or siTLE3 versus siCtl, or Drugs versus control, # FexD versus Vehicle in WT and $Apc^{Min/+}$ cohort, or T-βMCA versus FexD treatment, or Drug treatment after siTLE3 versus siTLE3. $ siTLE3 with FexD versus FexD only treatment. *, $^{\#}$, $^{\$}$ $P < 0.05$; **, $^{\#\#}$, $^{\$\$}$ $P < 0.01$; ***, $^{\#\#\#}$, $^{\$\$\$}$ $P < 0.005$; ns-not significant.

Notch signaling (Fig. S4F). Collectively, our data demonstrated that FXR mediates its tumor-suppressing effect partially by upregulating TLE3, a repressor of Wnt in ISCs.

In summary, our results demonstrate that the downregulation of TLE3 is common in CRC. FXR plays as a critical tumor suppressor partially through transcriptional upregulation of TLE3, thus inhibiting Wnt signaling in CRC. Therapeutic activation of FXR activity might be a novel strategy for Wnt-addicted CRC types, like secretory cell metaplasia.

Author contributions

T.F. conceived and designed the research. X.D., C.C., T.F. performed experiments and analyzed the results. X.D. conducted the western blotting and cell experiments. C.C. performed the immunostaining of TLE3 on tissue slides. T.F. conducted the ChIP experiment in cells and in mice, organoid and mice studies with FexD treatment. C.C. performed bioinformatic data analyses. T.F. drafted the manuscript, with all authors read and approved for the final manuscript.

Conflict of interests

The authors declare that they have no conflict of interests in this study.

Funding

This work is funded by UW-Madison startup grants for T.F. and is funded by American Cancer Society (ACS) Institutional Research Grant (IRG) (No. MSN228402).

Appendix A. Supplementary data

Supplementary data to this article can be found online at https://doi.org/10.1016/j.gendis.2022.09.006.

References

1. Medema JP, Vermeulen L. Microenvironmental regulation of stem cells in intestinal homeostasis and cancer. *Nature*. 2011; 474(7351):318—326.
2. Fu T, Coulter S, Yoshihara E, et al. FXR regulates intestinal cancer stem cell proliferation. *Cell*. 2019;176(5):1098—1112.
3. Thomas AM, Hart SN, Kong B, et al. Genome-wide tissue-specific farnesoid X receptor binding in mouse liver and intestine. *Hepatology*. 2010;51(4):1410—1419.
4. Villanueva CJ, Waki H, Godio C, et al. TLE3 is a dual-function transcriptional coregulator of adipogenesis. *Cell Metabol*. 2011; 13(4):413—427.
5. Liu L, Zhang Y, Wong CC, et al. RNF6 promotes colorectal cancer by activating the wnt/beta-catenin pathway via ubiquitination of TLE3. *Cancer Res*. 2018;78(8):1958—1971.

Xingchen Dong [1], Chunmiao Cai [1], Ting Fu *

Pharmaceutical Sciences Division, School of Pharmacy, University of Wisconsin Carbone Cancer Center (UWCCC), University of Wisconsin—Madison, Madison, WI 53705, USA

*Corresponding author. Pharmaceutical Sciences Division, University of Wisconsin—Madison, 777 Highland Ave, Madison, WI 53705, USA.
E-mail address: ting.fu@wisc.edu (T. Fu)

22 June 2022
Available online 4 October 2022

[1] These authors contributed equally to this work.